Pergamon

Cement and Concrete Research 33 (2003) 207–214

CEMENT AND CONCRETE RESEARCH

Using acoustic emission to quantify damage in restrained fiber-reinforced cement mortars

Byounggeon Kim, W. Jason Weiss*

School of Civil Engineering, Purdue University, 1284 Civil Engineering Building, West Lafayette, IN 47907-1284, USA

Received 4 January 2002; accepted 28 August 2002

Abstract

This paper describes the use of acoustic emission (AE) for monitoring early-age cracking in restrained fiber-reinforced mortars. A steel-testing frame was used to prevent the length reduction associated with drying. AE sensors placed on both unrestrained and restrained specimens detected a high degree of activity that may be attributed to surface microcracking caused by moisture gradients that cause the surface to shrink more rapidly than the core. It was found that as the concrete neared the age of visible cracking, the acoustic waves generated in the restrained specimens had a greater amplitude and duration. For this reason, acoustic energy was utilized for these investigations. An increase in acoustic energy was detected before cracks were observed in the restrained specimens. It is believed that the role of fiber reinforcement is twofold. First, fibers arrest cracks thereby preventing unstable crack propagation, and second, they restrain the crack from opening preventing the cracking from becoming visible until a later age.

Keywords: Crack detection; Fiber reinforced; Fracture toughness; Microcracking; Shrinkage

1. Introduction

Portland cement-based materials exhibit volume changes (shrinkage and expansion) as a result of temperature and moisture variations. If these length changes are prevented (restrained), residual stresses can develop. This is especially significant if moisture loss or temperature reduction is experienced, since these changes result in an overall reduction in length (i.e., shrinkage). The prevention of shrinkage by external restraint causes tensile stresses to develop that may be sufficient to cause cracking. These cracks may significantly reduce long-term durability by facilitating the accelerated ingress of aggressive agents. Recently, research on early-age shrinkage cracking has focused on assessing the level of residual stress that develops as a result of restraint [1–5] or on developing models to better understand how cracks develop [6–8]. This information has been used to develop analytical models to predict whether cracking should be expected and the severity of the cracks that may develop. However, further experimental data are needed to extend the analytical modeling formulations that are developed and to calibrate the models as they are implemented.

While the problem of predicting a materials cracking resistance is commonly simplified by assuming that moisture loss, shrinkage, and stress development occur uniformly across the cross section [9], it is widely known that this does not represent the actual physical behavior [9,10]. The presence of strong moisture and temperature gradients can result in the development of high stress levels near the surface of the concrete. Bazant and coworkers [11–13] and Granger et al. [14] have proposed that these stress gradients result in the development of microcracking at the surface of the concrete in both restrained and unrestrained specimens. The presence of these microcracks has recently been documented experimentally as well [15]. It is important to better understand how these microcracks form for two main reasons. First, these microcracks provide a source of stress relief thereby reducing the driving forces acting on the concrete to create new cracks. Second, these cracks provide potential sources for localized crack initiation and propagation that would be observed at later ages as visible "shrinkage" cracking. Currently however, little qualitative evidence

* Corresponding author. Tel.: +1-765-494-2215; fax: +1-765-496-1364.
E-mail address: wjweiss@ecn.purdue.edu (W.J. Weiss).

0008-8846/02/$ – see front matter © 2002 Elsevier Science Ltd. All rights reserved.
PII: S0008-8846(02)00978-X

exists to describe the process by which a single localized crack develops and propagates under restrained shrinkage conditions.

The potential for shrinkage cracking has increased with the use of higher strength concrete, especially if it is not sufficiently cured [16]. The correlation between increased cracking activity and increased strength has been attributed to a variety of factors including increased autogenous shrinkage, reduced creep, increased stiffness, and increased brittleness [17]. Several methods have been advocated to minimize the potential for cracking including using lower cement contents, improved curing conditions, expansive additives, or shrinkage reducing admixtures [6,18–20]. These approaches focus on reducing the shrinkage in concrete, thereby reducing the level of residual stress that develops [21]. Over the years however, several reports have shown that fiber reinforcement can delay the age of cracking and reduce the crack widths that develop [20–22]. It can be argued that low volumes of fiber reinforcement do not significantly alter the free shrinkage of concrete. Rather, fiber reinforcement must play another role. Restrained "ring tests" have shown a delay in the age of the first visible cracking when a sufficient volume of fiber is used [7]. It should however be noted that these specimens did show discontinuities in the residual strain level (as detected using surface mounted strain gages) before visible cracks were observed. Despite these observations, little work has quantitatively determined the specific mechanisms responsible for the improvements observed with fiber reinforcement.

2. Research significance

The objective of the current research was to assess whether acoustic emission (AE) can be used to quantify the mechanisms associated with cracking in fiber-reinforced materials. Specifically, this work will explore the hypothesis that the role of fiber reinforcement is to arrest cracking and to keep the crack width low, thereby delaying the age at which visible cracking may be observed. By better understanding the process of crack development, it is believed that fiber-reinforced composites can be better designed to improve their overall performance. Furthermore, it is believed that by better understanding the fracture processes, numerical simulation procedures can be improved thereby increasing the accuracy of performance predictions and enabling their use for life-cycle modeling applications.

3. Experimental procedures

The experiments described in this study were performed using standard concrete mortars prepared with a water-to-cement ratio (w/c) of 0.5 by mass. Fifty percent of the volume was composed of water and cement while 50% of the volume consisted of the "inert" components (fine aggregate and fiber reinforcement). The binder was an ordinary type I Portland cement (C_3S of 60%, C_2S of 13.5%, C_3A of 8.2%, Na_2O equivalent alkali content of 0.54%, the fineness of 360 m^2/kg). Fine steel fibers were used in this study with a length of 13 mm, diameter of 0.16 mm, and an elastic modulus of 210 GPa. Each mixture was mixed in a standard Hobart mixer in accordance with standard mortar procedures (ASTM C-305). Mixtures will be denoted in this paper by the volume of fiber reinforcement that was used (0%, 0.3%, 0.5%, 0.7%, and 1.0%).

Three different specimen geometries were used during this study, each of which had an identical drying surface to volume ratio (in the region of interest) thereby allowing the specimens to be directly compared with one another. Fig. 1 illustrates the specimen geometries for the restrained and unrestrained prisms that were used for the AE tests. Both specimens (restrained and unrestrained) used for AE testing had a 25 mm (1 in.) square cross section. Plastic notches were placed in the specimen at the time of casting at a distance of 50 mm (2 in.) from the center of the specimen to create a weak zone where visible cracking could be expected to occur. This was intended to improve the possibility of locating any visible cracking when the specimens were assessed daily. The depth of each notch was 3.1 mm (1/8 in.) while their aperture was 1 mm (0.04 in.). Two 275-mm (11 in.) long unnotched, unrestrained specimens were used to assess the free shrinkage and weight loss (similar to ASTM C-157 with sealed sides). Steel gage studs were placed at each end of the specimen during casting to facilitate length change measurements. The two sides and ends of all of the specimens were sealed to permit drying from only the top and bottom surfaces of the mortar specimens ($25 \times 25 \times 250$ mm).

The fresh mortar was placed in the forms, vibrated, sealed with an acrylic sheet, and stored under wet burlap at room temperature 23 ± 1 °C for 24 h. The specimens were then demolded. The free shrinkage specimens were removed from their formwork completely, while the restrained specimen was kept in the restraining steel frame as shown in Fig. 1. The two sides and two ends of the specimen were sealed with aluminum tape at the time of demolding to permit drying from only two surfaces (top and bottom). The specimens were then placed in an environmental chamber, which maintained the temperature at 23 ± 1 °C and the relative humidity at 50 ± 2%. The restrained specimens were monitored daily for signs of visible cracking at the reduced section using a hand-held magnifying glass.

In the specimens where acoustic activity was monitored, piezoelectric sensors were placed on the surfaces of the specimen (on the sealed side) as shown in Fig. 1. The sensors discussed in this paper were placed in the center of the restrained and unrestrained specimen. Two additional sensors were placed at either end of the restrained specimen to permit crack location information to be obtained for later analysis [23]. The distance from the notch to the central sensor was 50 mm (2.0 in.) for all specimens. This differs

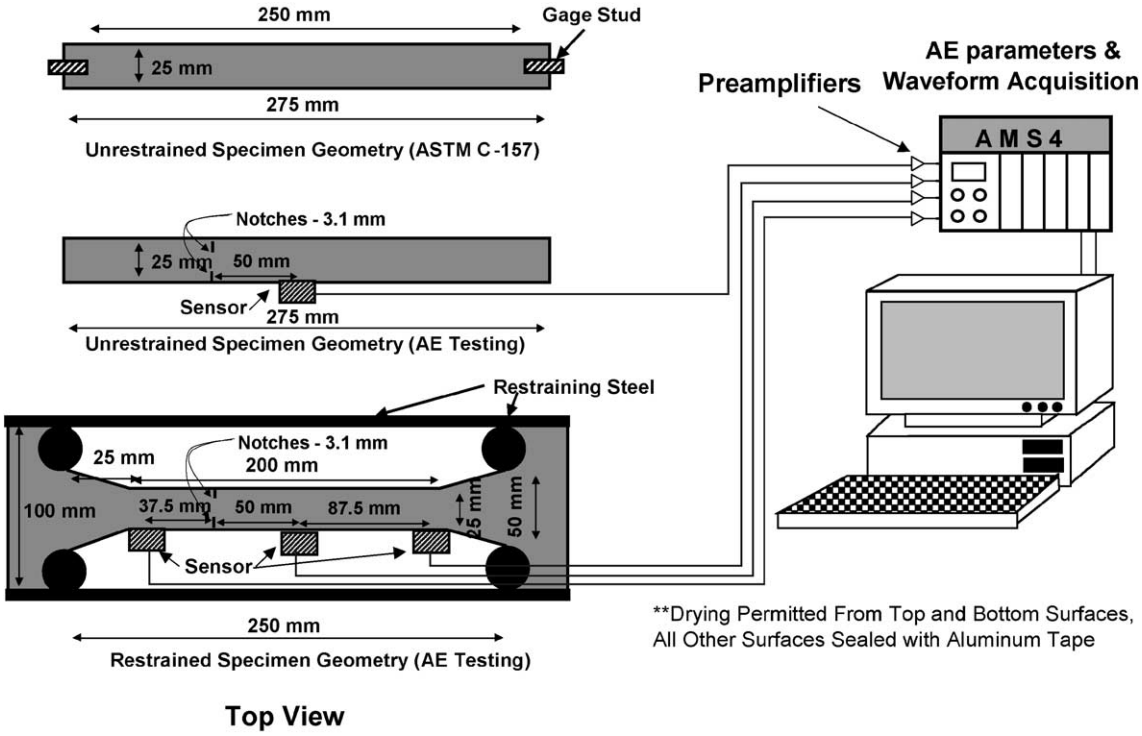

Fig. 1. Illustration of test specimen configuration.

from preliminary work where the sensors were placed on the drying surfaces of the specimen [23]. This change facilitated additional sensors to be located along the specimen without reducing the drying surface area thereby improving the accuracy and resolution for determining crack location. In addition, since the speed of waves in concrete can change due to drying effects, the change in sensor location was intended to aide in minimizing any losses due to wave propagation through a drying region.

A Vallen AMSY4 AE system was used throughout this investigation. Four broadband transducers were attached directly to the concrete surface using stiff vacuum grease as a coupling agent. Rubber bands were placed around the transducers to supply a light mechanical force to keep the sensor in contact with the specimen. These transducers were used to convert the detected waves into electrical signals, which were amplified, processed, and recorded using the Vallen Acquisition 32 software. Analysis of the recorded waves was performed using the Visual-AE software.

4. Experimental results and analysis

Fig. 2 provides an indication of the shrinkage and weight loss characteristics of the specimens described in this paper. It can be seen that the shrinkage is quite similar irrespective of the fiber volume; however, the specimens containing fibers showed a slightly higher weight loss. This increased

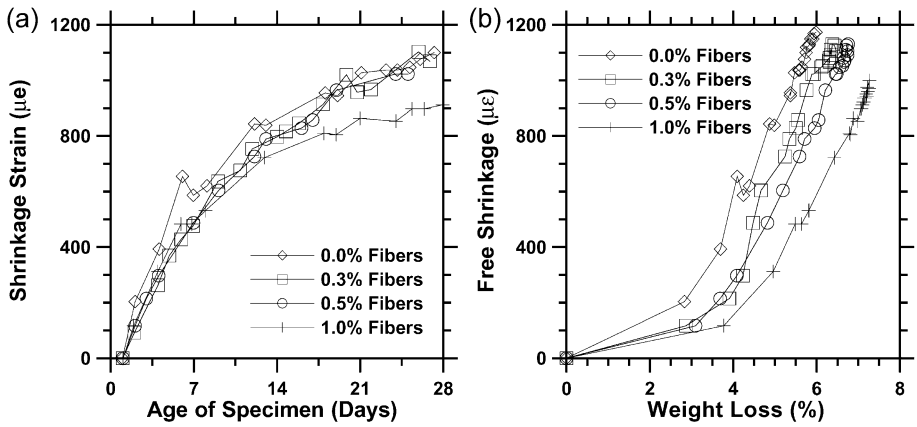

Fig. 2. (a) Drying shrinkage and (b) moisture loss.

weight loss was observed to be the most prominent at early ages and may be attributed to moisture movement along the porous region that forms at the surface of the fiber, however further research is needed to quantify this assumption. Consistent with previous studies [7,21], the restrained specimens showed a delay in the age of visible cracking as the fiber volume increased. Table 1 provides a summary of the age when cracking was observed as well as the previous age when the specimen was monitored prior to the observation of visible cracking. It can be seen that the specimens containing an addition of 1.0% fibers did not develop any visible cracking when testing was stopped after 21 days.

In addition to the measurements of length and weight change, acoustic activity was recorded as described in the following section. Several different AE parameters will be used to describe the behavior of the restrained mortars [24]. To better understand these parameters, a typical waveform is presented in Fig. 3. Several features of this waveform (hit) will be discussed in this paper including the amplitude, duration, and energy. The term "acoustic hit" (or acoustic event) describes a burst of acoustic activity once by recognizing the beginning and end of each discrete burst. The beginning of each acoustic hit (or event) is indicated when the amplitude of the signal from the transducer exceeds some threshold value. The end of each hit is determined as the time the signal amplitude decreases below the threshold limit for the last time. The amplitude of the signal refers to the maximum absolute value of the signal recorded while duration refers to the time during which the signal remains above the threshold. This paper will use these acoustic parameters to better describe the crack development and propagation process in restrained concrete. Further information on these measurements is provided in the following section, while the concept of acoustic energy will be described later in the paper as it is used.

The first approach discussed in this paper investigates the number of acoustic hits (sometimes called acoustic events) generated during each test. A cumulative plot of the acoustic hits versus time for the restrained and unrestrained specimens (center sensors) is provided in Fig. 4. It can be seen that acoustic activity is measured immediately upon placing the sensor on the specimen and placing the specimen in the drying environment (1 day). It should be noted that the

Table 1
Age of cracking

Fiber volume (%)	Last visual observation before cracking (days)	First visual observation after cracking (days)	Cracking as determined with AE (days)
0.0	2.0	3.0	2.5
0.3	4.0	4.9	4.0
0.5	4.0	5.1	5.1
0.7	10.9	11.9	9.5
1.0	20.0	–	~16

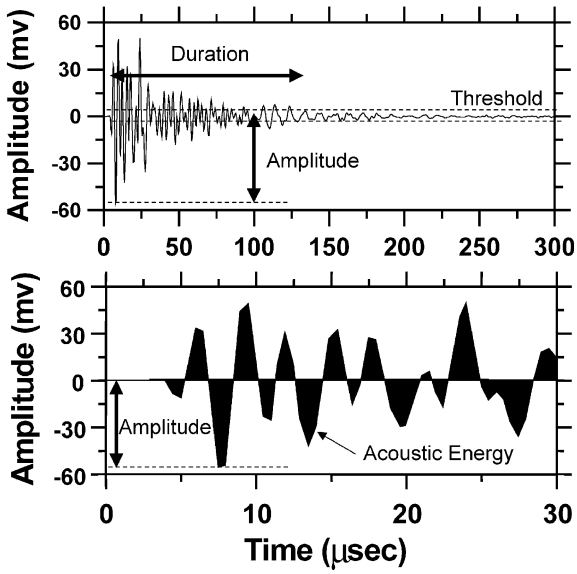

Fig. 3. Illustration of a typical waveform measured and the acoustical parameters used in this paper.

specimens were placed in the drying environment and data acquisition was begun within 20 min of the start of the demolding process. As such, any acoustic activity that occurs before this time was not measured in this investigation. The data in Fig. 4 show that initially the number of hits measured in the unrestrained and restrained specimens is very similar for both the plain and reinforced specimens. Fig. 4a illustrates that for plain mortar, the cumulative hits measured in the restrained and unrestrained plain specimens diverge at an age of approximately 2 days. This corresponds to a discrete increase in acoustic activity and the development of a visible crack on the surface of the restrained specimen. At this time, it should be noted that the sudden increase in energy is noticed in specimens with an initial notch while unnotched specimens show a more gradual increase at a later age [23]. Fig. 4b illustrates the behavior of a fiber-reinforced specimen (0.7% fibers). Again, it can be seen that similar behavior is observed between the restrained and unrestrained specimens. It can also be noticed, however, that the more heavily reinforced restrained specimens do not show a discrete rise in acoustic hits at any age, despite the fact that small visible cracks were observed on the surface of the restrained specimen (at an age of 12 days for the case of 0.7% fibers). This is important because it shows that acoustic hits alone cannot provide a complete description of the cracking behavior.

At this time, it should be noted that the use of the parameter "hits" only provides an indication of the number of "burst emissions" or "events" and does not describe the quality or magnitude of the acoustic events. As a result, further analysis was performed to quantify the magnitude of the acoustic events. Fig. 5 shows the amplitude of all of the waves generated in the restrained and unrestrained specimens (0.7% fiber). It can be seen (0.7% fiber shown) that

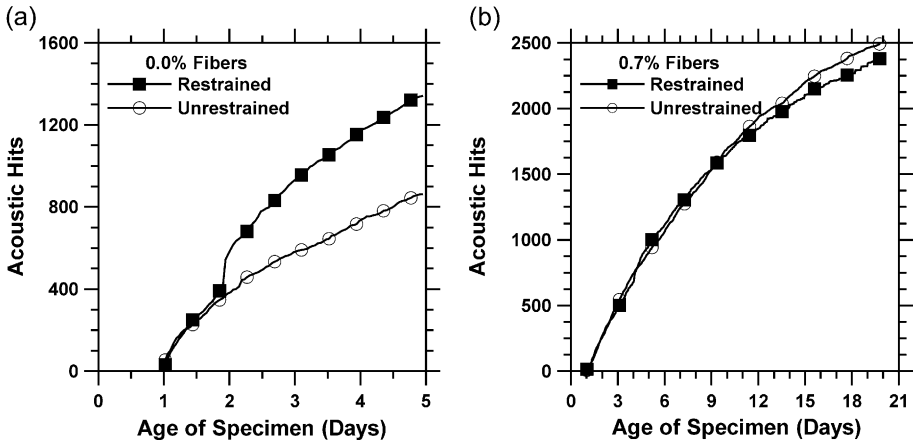

Fig. 4. Comparison of acoustic hits (events) for the restrained and unrestrained specimen with (a) 0% fibers and (b) 0.7% fibers.

the unrestrained specimens demonstrate events that are typically below 50 dB and have a high concentration of hits below 40 dB. The restrained specimens, however, show a significant number of higher amplitude events. These high-amplitude events occur especially after an age of approximately 9 days for the 0.7% fiber case although this time will vary depending on the mixture composition. Additional comparison of the duration of the acoustic hits for the unrestrained and restrained specimens indicated longer duration events in the restrained specimens at later ages. This information provides an important distinction between the behavior of mortar in the free and restrained specimen. At early ages, the number and quality of the acoustic events are similar, thereby suggesting that little difference should be expected in the cracks that develop in the restrained and unrestrained specimens. As the drying time increases, the magnitude of the acoustic waves generated in the restrained specimens increases, thereby suggesting the development of more substantial (larger) cracks in the restrained specimen. This may perhaps be caused by the penetration of cracks further into the core of the specimen or the development of cracking along the length of the fiber, however, further studies would be needed to validate these hypotheses.

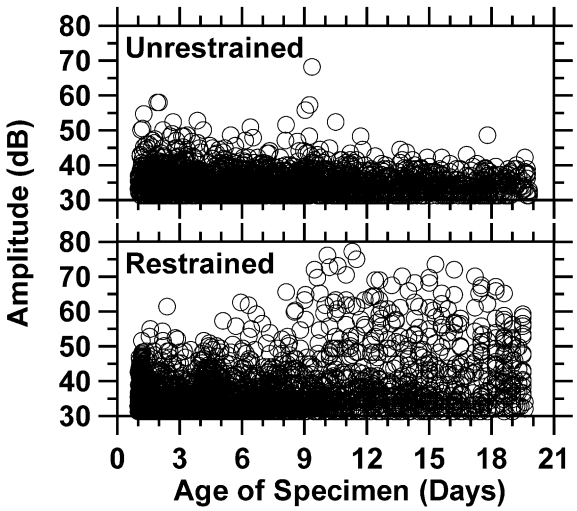

Fig. 5. Comparison of the amplitude of the acoustic hits (events) for unrestrained and restrained specimens (0.7% fibers).

For this reason, it is proposed that a parameter other than hits should be used to provide a better indication of differences in the waves. The parameter that was chosen for the remainder of this study is acoustic energy. As shown in Fig. 3, acoustic energy (in this paper) describes the absolute value of the integral of the voltage versus time for each hit. This provides a parameter that accounts for the change in amplitude and duration of the events. In addition, recent research by Landis and Ballion [25] has shown that the acoustic energy may be proportional to the mechanically measured fracture energy. Fig. 6 shows the cumulative acoustic energy versus time (recorded by the center sensor) in the restrained and the unrestrained specimens. Immediately upon drying, the acoustic energy measured in the plain specimens demonstrate similar behavior (Fig. 6a). At an age of 2 days, a rapid increase in acoustic energy can be observed in the restrained specimen. This is consistent with the increase in acoustic hits, the occurrence of a few high-amplitude, long-duration events, and the development of a visible crack. Fig. 6b provides a similar plot of cumulative energy versus time for a 0.7% fiber-reinforced specimen. Again, it can be seen that during the first 2–3 days of drying, the restrained and unrestrained specimens demonstrate a similar response. After this time, the total energy measured in both specimens begins to diverge. The restrained specimen shows an increase in the rate of acoustic energy dissipation measured between the ages of 3 and 9 days. After an age of 9 days, an additional increase in the rate of acoustic energy is observed. It should be noted that the rate of energy release does not change when the crack becomes visible (0.7%, 11–12 days) as one may expect based on the results of the plain mortar tests. This suggests the possibility that a through crack may have actually occurred at an earlier age. For example, the 0.7% fiber-

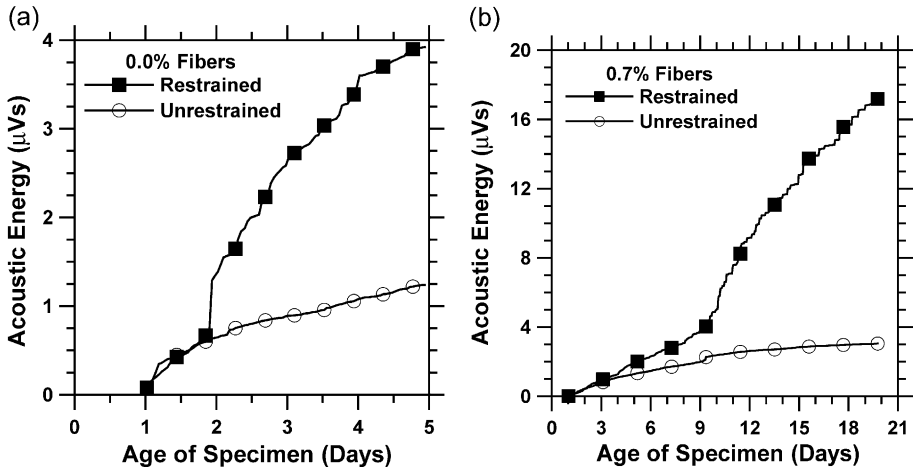

Fig. 6. Comparison of acoustic energy measured in the restrained and unrestrained behavior of (a) plain (i.e., 0% fiber) and (b) fiber-reinforced specimens (0.7% fibers).

reinforced specimen shows a change in energy release rate at 9.5 days while cracking became visible at 11.9 days. The delay between the age of the specimen when an increase in energy release rate occurs (9 days) and when visible cracking (11.9 days) occurs may be attributed to the fibers ability to redistribute stress, transfer stress across the crack, and bridge the crack to keep the crack below a width that is visible to the human eye (50–100 μm). Fig. 7 shows a comparison of the acoustic energy measured in each specimen containing various volumes of fibers. It can be seen that all of the specimens demonstrate a similar energy release rate, however it can be noticed that as the fiber volume increases the rate decreases slightly. Further testing will be needed to assess the statistical significance of these differences. It can also be seen that the fiber-reinforced specimens consume a greater amount of energy before cracks become visible. This would be consistent with the fact that the toughness (fracture energy) of a specimen increases with increasing fiber volume [22,26].

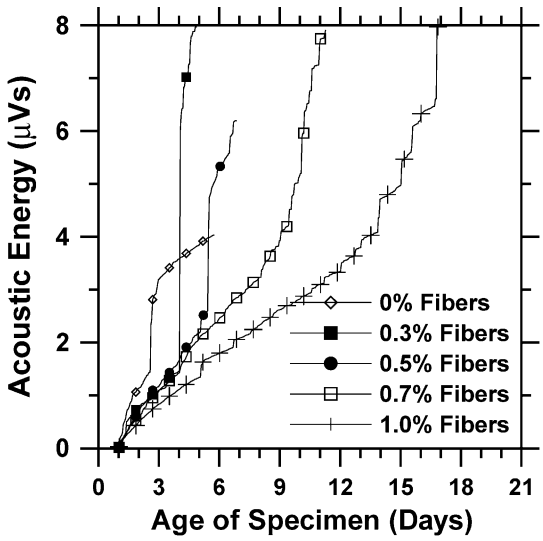

Fig. 7. Acoustic energy comparison for various fiber volumes.

Fig. 7 also shows that the discrete rise in acoustic energy that occurs when cracks become visible for the plain (low fiber volume) specimens begins to become more gradual for the higher fiber volume specimens. Soon after visible cracking is observed in the specimens without fibers, an acoustic energy release is observed that is similar to the unrestrained specimens. This is not true for the fiber-reinforced specimens though. This is significant in that it suggests that in the plain specimen the crack has propagated through the specimen creating two "unrestrained" specimens. This is not observed in the fiber-reinforced specimens however, since even after the visible crack is observed the fibers bridge the crack thereby maintaining a tensile stress in the specimen.

As previously mentioned, the amplitude and duration of the waves measured in the restrained specimen change as the specimen nears the age of visible cracking. Fig. 8 divides the total energy measured into percentage of energy recorded in various amplitude ranges for the unrestrained and restrained specimen. It can be seen that the unrestrained specimens have a relatively constant percentage of energy recorded in each amplitude range over time (Fig. 8a), while the acoustic energy measured in each amplitude range of the restrained specimen varies over time with a substantial increase in high amplitude events (for 0.7% fibers this occurs at 9–10 days).

The AE information can also be used to try to improve our understanding of how cracks initiate and propagate under restraint. Fig. 9 illustrates the acoustic energy release rate (the numerical derivative of the acoustic energy). It can be seen that initially the plain specimen had a high rate of energy release, which is most likely attributed to the drastic "shock" associated with the high surface area of the material suddenly being exposed to severe drying and the corresponding cracks that develop. The AE energy rate then

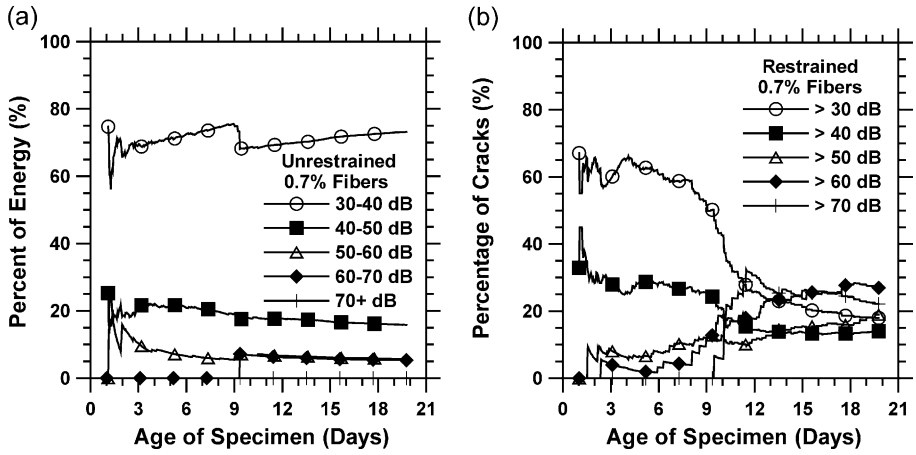

Fig. 8. Comparison of acoustic energy attributed to events of each amplitude range in the restrained and unrestrained specimens for (a) 0% fibers and (b) 0.7% fibers.

decreases and levels off until a sharp peak is observed at the time the crack becomes visible. The specimens containing higher volumes of fiber show a similar decrease in rate initially, however several spikes (discrete increases) of acoustic energy release can be seen before visible cracking is observed. Low fiber volume mixtures show similar, albeit fewer, spikes.

It is currently believed that these discrete jumps in the energy release rate in the fiber-reinforced specimen may be explained in part by the fibers acting to arrest cracks before they propagate across the specimen. A conceptual illustration of this idea is presented in Fig. 10. This figure illustrates that immediately upon drying microcracks will begin to develop at the surface of the concrete [13–15]. Once this crack reaches some critical length in the plain restrained mortars, unstable cracking would be expected to occur and a visible crack would be expected to appear. However, it is speculated that when this crack begins to grow in a fiber-reinforced specimen, it is arrested by a fiber (Fig. 10b), thereby requiring a greater driving force to propagate across the specimen. In low volume composites, the propagation of this crack would result in the development of a visible surface crack. However, at higher fiber volumes, it is believed that the fibers act to bridge the crack (Fig. 10c), thereby making it difficult to locate the crack. As a result, additional loading (time) is needed for this crack to open to a significant width to where it becomes visible to the human eye. Further research is needed to validate these ideas using a combination of microscopy with acoustic monitoring.

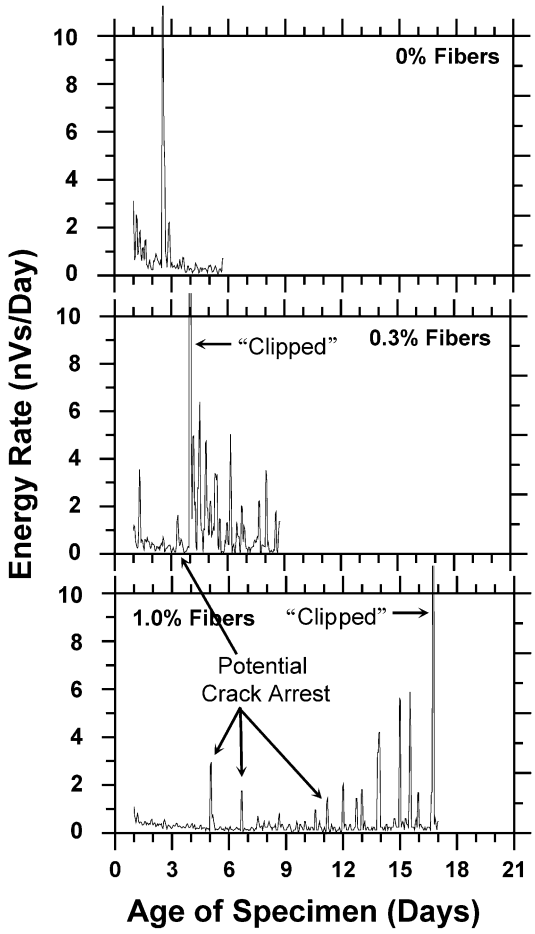

Fig. 9. AE energy release rate for 0%, 0.3%, and 1.0% fibers.

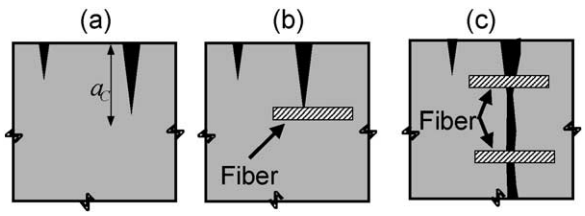

Fig. 10. A conceptual illustration of the role of fiber reinforcement.

5. Summary

In summary, this paper does not claim to have explained all aspects of early-age cracking in fiber-reinforced mortars that are restrained from shrinking freely. It has however shown that AE may have the potential to be used to quantify damage that occurs in restrained cementitious materials. Acoustic activity was measured in both the reinforced and unreinforced specimens. Comparing the acoustic hits (events) may provide a method to indicate the time of cracking in plain specimens, however in fiber-reinforced specimens the time of cracking may not be assessed using hit information alone. It was illustrated that the characteristics of the waves generated at the time of cracking generally illustrate a shift from low-amplitude short-duration signals to higher amplitude–longer duration signals near the time of cracking. Measurement of AE energy (the area under the waveform curve) may provide a better indication of the time of cracking, while the rate of AE energy release may provide information as to the development and propagation of a localized crack.

Acknowledgements

The authors acknowledge support received from the Purdue Research Foundation, the Center for Advanced Cement-Based Materials (Project C-1), and the Institute for Safe, Quiet, and Durable Highways (SQDH). In addition, the authors gratefully acknowledge support from the Charles Pankow Concrete Materials Laboratory.

References

[1] S.A. Altoubat, D.A. Lange, Early-age creep and shrinkage of fiber reinforced concrete for airfield pavement, in: F.V. Hermann (Ed.), Aircraft Pavement Technology, ASCE, New York, 1997, pp. 229–243.
[2] R. Bloom, A. Bentur, Free and restrained shrinkage for normal and high strength concretes, ACI Mater. J. 92 (2) (1995) 211–217.
[3] A.M. Parilee, M. Buil, J.J. Serrano, Effect of fiber addition on the autogenous shrinkage of silica fume concrete, ACI Mater. J. 86 (2) (1989) 139–144.
[4] K. Kovler, Testing system for determining the mechanical behavior of early age concrete under restrained and free uniaxial shrinkage, Mat. Struct., vol. 27(170), RILEM, London, UK, 1994, pp. 324–330.
[5] E. Sellevold, Report 2.4: Mechanical properties of young concrete: evaluation of test methods for tensile strength and modulus of elasticity. Determination of model parameters. NOR-IPACS Report, SINTEF (1999), 45 pp.
[6] G. Toma, M. Pigeon, J. Marchand, B. Bissonnette, L. Bercelo, Early-age autogenous restrained shrinkage: stress build up and relaxation, in: B. Persson, G. Fagerlund (Eds.), Self-Desiccation and Its Importance in Concrete Technology, Lund University, Proceedings of the Second International Research Seminar in Lund, Lund, Sweden, 1999, pp. 61–72.
[7] M. Gryzbowski, S.P. Shah, Model to predict cracking in fiber reinforced concrete due to restrained shrinkage, Mag. Concr. Res. 41 (148) (1989) 125–135.
[8] W.J. Weiss, W. Yang, S.P. Shah, Shrinkage cracking of restrained concrete slabs, ASCE J. Eng. Mech. 124 (7) (1998) 765–774.
[9] W.J. Weiss, W. Yang, S.P. Shah, Influence of specimen size/geometry on shrinkage cracking of rings, ASCE J. Eng. Mech. 126 (1) (2000) 93–101.
[10] F.H. Wittman, Deformation of concrete at variable moisture content, (Chapter 19), in: Z.P. Bazant (Ed.), Mechanics of Geomaterials, Wiley, New York, 1985, pp. 425–459.
[11] Z.P. Bazant (Ed.), Fourth RILEM International Symposium on Creep and Shrinkage of Concrete: Mathematical Modeling, Northwestern University, Evanston, IL, USA, August 26–29.
[12] Z.P. Bazant, A.B. Wahab, Instability and spacing of cooling or shrinkage cracks, ASCE J. Eng. Mech. 105 (1979) 873–889.
[13] Z.P. Bazant, J.C. Chern, Concrete at variable humidity: constitutive law and mechanisms, Mat. Struct. 18 (1985) 1–20 (January, RILEM, Paris).
[14] L. Granger, J.M. Torrenti, P. Acker, Thoughts about drying shrinkage: experimental results and quantification of structural drying creep, Mat. Struct. 30 (1997, December), 588–598.
[15] J. Bisschop, J.G.M. van Mier, Shrinkage microcracking in cement-based materials with low water–cement ratio, in: K. Kovler, A. Bentur (Eds.), RILEM International Conference on Early Age Cracking in Cementitious Systems, EAC'01, Haifa, Israel, 2001.
[16] P.-C. Aitcin, Autogenous shrinkage measurement, in: E. Tazawa (Ed.), Autoshrink '98, Proceedings of the International Workshop on Autogenous Shrinkage of Concrete, Hiroshima, Japan, E & FN Spon, New York, 1988, pp. 245–256.
[17] W.J. Weiss, W. Yang, S.P. Shah, Factors influencing durability and early-age cracking in high strength concrete structures, ACI Special Publication 186, High Performance Concrete: Research to Practice, ACI Farmington Hills, MI, 1999, pp. 387–409.
[18] K. Van Breugel, J. de Vries, Mixture optimization of low water/cement ratio high strength concretes in view of autogenous shrinkage, International Symposium on High Performance and Reactive Powder Concrete, Sherbrooke, Canada, 1998, pp. 365–382.
[19] E. Tazawa (Ed.), Autoshrink-98, Proceedings of the International Workshop on Autogenous Shrinkage of Concrete, Japan Concrete Institute, Hiroshima, Japan, E & FN Spon, New York, June 13–14. 358 pp.
[20] C. Nmai, R. Tomita, F. Hondo, J. Buffenbarger, Shrinkage reducing admixtures, Concr. Int. 20 (4) (1998) 31–37.
[21] S.P. Shah, W.J. Weiss, W. Yang, Shrinkage cracking—can it be prevented? Concr. Int. 20 (4) (1998, April), 51–55.
[22] P.N. Balagaru, S.P. Shah, Fiber Reinforced Composites, McGraw-Hill, New York, 1992. 530 pp.
[23] T. Chariton, W.J. Weiss, ACI Special Publications 206, Concrete: Material Science to Application, in: P. Balaguru, A.E. Naaman, W.J. Weiss (Eds.), A tribute to Surrendra P. Shah, Farmington Hills, Michigan, 2002, pp. 205–218.
[24] S. Mindess, Acoustic emission methods, (Chapter 14), in: V.M. Carino, N.J. Carino (Eds.), CRC Handbook on Non Destructive Testing of Concrete, CRC Press, Boca Raton, FL, 1991, pp. 317–334.
[25] E. Landis, L. Ballion, Experiments to relate acoustic energy to fracture energy of concrete, J. Eng. Mech. 128 (2002) 698–702.
[26] D.J. Hannat, Fibre Cements and Fibre Concretes, Wiley, New York, 1978.